

# Coupled-Channel and Screening Effects in Charmonium Spectrum

Bai-Qing Li<sup>a,b</sup>, Ce Meng<sup>a</sup> and Kuang-Ta Chao<sup>a</sup>

<sup>a</sup>*Department of Physics and State Key Laboratory of Nuclear Physics and Technology,  
Peking University, Beijing 100871, China;* <sup>b</sup>*Department of Physics,  
Huzhou Teachers College, Huzhou 313000, China*

(Dated: November 3, 2018)

Using the same quenched limit as input, we compare the charmonium spectra predicted by the coupled-channel model and the screened potential model in the mass region below 4 GeV, in which the contributions from decay channels involving P-wave (as well as even higher excited) D mesons can be neglected. We find that the two models have similar global features in describing charmonium spectrum since they embody the same effect of the vacuum polarization of dynamical light quark pairs. This agreement is encouraging for using the screened potential to further describe the mass spectrum of higher charmonium in the region above 4 GeV. Applying both models will be helpful to clarify the nature of the newly discovered "X, Y, Z" mesons in B-factories and other experiments. In particular, we show the S-wave decay coupling effect on lowering the  $\chi_{c1}(2P)$  mass towards the  $D\bar{D}^*$  threshold, in support of the assignment of the X(3872) as a  $\chi_{c1}(2P)$ -dominated charmonium state.

PACS numbers: 12.39.Jh, 13.20.Gd, 14.40.Gx

## I. INTRODUCTION

Studies on heavy quarkonium spectroscopy have been stimulated greatly in recent years by the discovery of many hidden charm states, the so-called "X, Y, Z" mesons [1] in B-factories and other experiments. The QCD-inspired interquark potential models, such as the Cornell model [2], are successful in predictions of charmonium and bottomonium spectra below the open flavor thresholds. However, the existence of open charm thresholds can change the charmonium spectrum significantly through the virtual charm meson loops. These coupled-channel effects were considered also in the Cornell model [2], and techniques were further developed by the unitaritized quark model [3] based on the  $^3P_0$  quark pair creation model [4]. Along this line and with the updated parameters, the coupled-channel effects in the charmonium spectrum have been further studied during these years [5, 6, 7]. These studies provide important information on the identifications of the "X, Y, Z" mesons.

The quark potential model is subject to modification due to quantum fluctuation, i.e., the creation of light quark pairs, which may be compensated by the virtual hadron loops in the coupled-channel model. For this reason, the quark potential model [2], which incorporates a Coulomb term at short distances and a linear confining term at large distances, may be called as the quenched potential model. On the other hand, the vacuum polarization effect of the dynamical fermions may soften the linear potential at long distances [8], and cause the screening effect, which may be discussed phenomenologically as the screened potential model [9, 10, 11]. Such screening or string breaking effects have been demonstrated, although indirectly, by the simulations of unquenched lattice QCD [12]. This effect is also implied by calculations within some holographic QCD models [13]. The screened potential model has been used to reexamine

the charmonium spectrum [14] recently, and it is found that the masses of higher charmonium states are lowered, compared to the quenched potential model [15], and the mass suppression tends to be strengthened from lower levels to higher ones. Such tendency can also be found in the calculations of the coupled-channels model, such as those in Ref. [6]. It is not very surprising since, in the parton-hadron duality picture, the two models embody the same effects of light quark pairs.

Comparing to the screened potential model, the coupled-channel model is more difficult to handle in practice, especially in the case when the P-wave (and higher excited)  $D$  and  $D_s$  mesons as the intermediate states are involved. However, the latter can describe the near-threshold effect [6, 7, 16], which has been ignored in the former. It is then interesting to compare the two models using the same quenched limit as input in the domain of charmonium spectrum. The comparison has twofold meaning: the coupled-channel model can be helpful to establish the form of the screened potential and to determine the screening parameter  $\mu$  in the mass region below 4 GeV, where the P-wave  $D$  mesons are expected to be decoupled; whereas the screened potential model can be helpful to normalize the global features of the coupled channel model in the mass region above 4 GeV.

In this paper, we will compare these two models in the mass region below 4 GeV for charmonium spectrum with the same quenched limit. We will introduce the two models in turn. And we will compare results of these two models numerically, and finally a summary will be given.

## II. QUENCHED AND SCREENED POTENTIAL MODELS

We choose the Cornell model [2] as the quenched limit, in which the potential has the well known form:

$$V(r) = -\frac{4}{3} \frac{\alpha_c}{r} + \lambda r + C, \quad (1)$$

where the first term denotes the color Coulomb force in the one-gluon exchange approximation due to asymptotic freedom of QCD at short distances, and the second term denotes the linear confining potential, which is consistent with both the rotating string picture [17] and the quenched lattice calculations (see [18] for a review and references). The constant  $C$  in (1) is the renormalization term.

In principle, one can relate the parameter  $\alpha_c$  to the running coupling constant  $\alpha_s(m_{cv})$  in QCD, where  $v^2 \approx 0.3$  is the charm quark velocity squared in the charmonium rest frame, and relate  $\lambda$  to the string tension  $T = 1/(2\pi\alpha') \sim 0.18 \text{ GeV}^2$ , where  $\alpha'$  denotes the Regge slope in the rotating string picture [17]. Thus, we choose

$$\alpha_c = 0.55, \quad \lambda = 0.175 \text{ GeV}^2 \quad (2)$$

in the following analysis.

To restore the hyperfine and fine structures of the charmonium spectrum, one needs to introduce the spin-dependent potential  $V_{sd}$ , which is relativistically suppressed compared to  $V$  in (1). Assuming the Lorentz structure of the linear confining force is of scalar type, the spin-dependent potential can be derived from (1) by the standard Breit-Fermi expansion to order  $v^2/c^2$ , and has the form [15]

$$V_{sd}(r) = \left( \frac{2\alpha_c}{m_c^2 r^3} - \frac{\lambda}{2m_c^2 r} \right) \vec{L} \cdot \vec{S} + \frac{32\pi\alpha_c}{9m_c^2} \tilde{\delta}(r) \vec{S}_c \cdot \vec{S}_{\bar{c}} + \frac{4\alpha_c}{m_c^2 r^3} (\vec{S}_c \cdot \vec{S}_{\bar{c}} + \frac{3(\vec{S} \cdot \vec{r})(\vec{S} \cdot \vec{r})}{r^2}). \quad (3)$$

where  $\vec{S} = \vec{S}_c + \vec{S}_{\bar{c}}$  is the total spin,  $m_c$  the charm quark mass, and the smeared delta function is taken to be  $\tilde{\delta}(r) = (\sigma/\sqrt{\pi})^3 e^{-\sigma^2 r^2}$  with  $\sigma = 1.45 \text{ GeV}$  [15]. Then, the Hamiltonian for the quenched potential model is given by

$$H_0 = 2m_c + \frac{\vec{P}^2}{m_c} + V(r) + V_{sd}(r), \quad (4)$$

where the kinematic energy term have been included explicitly.

As mentioned above, the linear confining potential will be softened by the vacuum polarization induced by the dynamical quark pair creation. Such unquenched effect can be roughly accounted for by modifying the long distant behavior of  $V(r)$  in (1). Following Refs. [10, 11], we use the screened potential

$$V_{scr}(r) = -\frac{4}{3} \frac{\alpha_c}{r} + \lambda r \frac{1 - e^{-\mu r}}{\mu r} + C \quad (5)$$

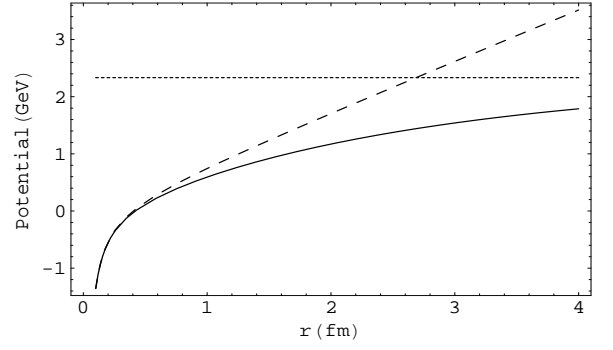


FIG. 1: Comparison of the Cornell potential  $V(r)$  (dashed line) and the screened potential  $V_{scr}$  (solid line) with  $r = 0.1-4$  fm. The constant terms are neglected and asymptotic limit of  $V_{scr}$  is shown in the dotted line.

to substitute  $V(r)$ . The first term on the right-hand side of (5) is taken to be the same as that in (1) due to its short distance nature. The screening parameter  $\mu$  sets the scale of distance at which the string breaks. We choose

$$\mu = 0.075 \text{ GeV}, \quad (6)$$

of which the inverse is about two times of the radius of  $D$  meson. Needless to say, the right hand side of (3) should also be modified accordingly.

At short distances, the screened potential  $V_{scr}$  in (5) has the limit consistent with that of  $V(r)$  in (1). However, the difference between the potentials increases when  $r$  increases, and finally  $V_{scr}$  goes to a constant  $\lambda/\mu + C$  when  $r \rightarrow \infty$ , as shown in Fig. 1. As a result, the charmonium spectrum in the screened potential model will be suppressed compared to that in the quenched potential model, especially for the higher excited states. Furthermore, in the screened charmonium spectrum, there will be a saturation energy of about 5-6 GeV, at which the  $c\bar{c}$  quark pair can not be bound together at all.

Let's stress again that the parameters in (2) and (6) may not be the same as those chosen in [14], since our purpose here is to compare the spectra in the two models rather than to get a good fit of the spectrum to the experimental data.

## III. THE $^3P_0$ -BASED NON-RELATIVISTIC COUPLED CHANNEL MODEL

The light quark pair creation from vacuum is assumed to share the same quantum number,  $0^{++}$ , as the vacuum in the  $^3P_0$  model [4]. In the non-relativistic limit, the  $^3P_0$  model can be represented by the Hamiltonian [19]

$$H_{QPC} = 2m_q \gamma \int d^3\vec{x} \bar{\Psi}_q \Psi_q, \quad (7)$$

where  $m_q$  is the mass of the produced quark, and  $\gamma$  is a constant reflecting quark pair creation strength,

which can be determined phenomenologically by the OZI-allowed decay widths of charmonia [15]. There are no fundamental reasons to enhance the heavier quark creation relative to lighter ones, which is implied by the factor of  $2m_q$  in (7). Therefore, following Ref. [7], we use the effective strength  $\gamma_s = \frac{m_q}{m_s}\gamma$  for the strange quark, where  $\frac{m_q}{m_s}$  is the ratio of constituent masses of up and down quarks ( $m_q = m_u = m_d$ ) and strange quark ( $m_s$ ). Following Ref. [7], we choose  $\gamma = 0.322$ .

Light quark pair creation can result in mixing between the bare charmonium state  $\psi_0(c\bar{c})$  and the open charmed meson pair  $B(c\bar{q})$  and  $C(q\bar{c})$ . Thus, neglecting the mixing among the bare states [5], the physical state  $\Psi$  can be represented by

$$|\Psi\rangle = a_0 |\psi_0\rangle + \sum_{BC} \int d\nu c_{BC}(\nu) |BC; \nu\rangle, \quad (8)$$

where  $\nu$  denotes the variable of three-momenta of the  $BC$  system. The coefficients  $a_0$  and  $c_{BC}(\nu)$  are understood to be subject to the normalization of the corresponding wave functions.

The Hamiltonian of this coupled-channel system can be formally written as

$$H = H_0 + H_{BC} + H_{QPC}. \quad (9)$$

Here,  $H_0$  has been introduced in (4) but can be different from the one in the quenched potential model by different renormalization constant  $C$ . The Hamiltonians  $H_0$  and  $H_{BC}$  can only act on the states  $\psi_0$  and  $BC$ , respectively, and give the bare spectra of them:

$$H_0 |\psi_0\rangle = M_0 |\psi_0\rangle, \quad (10)$$

$$H_{BC} |BC\rangle = E_{BC}(\nu) |BC; \nu\rangle, \quad (11)$$

where  $M_0$  is the so-called bare mass of the bare charmonium state and

$$E_{BC}(\vec{P}_B, \vec{P}_C) = \sqrt{M_B^2 + \vec{P}_B^2} + \sqrt{M_C^2 + \vec{P}_C^2}, \quad (12)$$

provided that the inner interactions between  $B$  and  $C$  can be neglected. On the other hand, the  $H_{QPC}$  in (9), which is defined in (7), can act only between  $|\psi_0\rangle$  and  $|BC; \nu\rangle$ .

The Hamiltonian  $H$  in (9) defines the physical mass  $M$  of the state  $\Psi$  as

$$H |\Psi\rangle = M |\Psi\rangle, \quad (13)$$

and the mass  $M$  can be obtained by solving the multi-channel Schrödinger equation (13). Substituting (8)-(11) into (13), one can get the integral equation

$$M + \Pi(M) - M_0 = 0, \quad (14)$$

where the self-energy function  $\Pi(M)$  is given by

$$\Pi(M) = \sum_{BC} \int d\nu \frac{|\langle BC; \nu | H_{QPC} | \psi_0 \rangle|^2}{E_{BC}(\nu) - M + i\epsilon}. \quad (15)$$

When  $\text{Re}[M] > M_A + M_B$ , it is obvious that the function  $\Pi(M)$  will not be real, and the imaginary part is proportional to the decay width of  $\Psi \rightarrow BC$ . Therefore, one can solve Eq.(14) in the complex plane and get the pole mass  $\text{Re}[M]$  [6]. However, we will define the coupled-channel mass  $M_{cou}$  as [7]

$$M_{cou} + \text{Re}[\Pi(M_{cou})] - M_0 = 0, \quad (16)$$

which is also called the Breit-Wigner mass by the authors of Ref. [6].

It is worth emphasizing here the difference between the definitions of the bare mass in [6] and of ours. The authors of Ref. [6] once subtract the dispersion integral in (15) at  $M_\psi$ , and absorb the term  $\Pi(M_\psi)$  into the bare mass definition:

$$M'_0 = M_0 - \Pi(M_\psi), \quad (17)$$

where  $\Pi(M_\psi)$  is real and positive, which can be seen directly from the definition of the function  $\Pi(M)$  in (15). If the subtracted constant  $\Pi_n(M_\psi)$  are the same for all the charmonium states  $n$ , the bare mass  $M'_0$  in (17) is just a rescaling one of  $M_0$  and the renormalized mass shift would not be changed. In Ref. [6], the matrix element square  $|\langle BC | H_{QPC} | \psi_0 \rangle|^2$  in (15) is simply parameterized by using an exponential form factor, and the node structure in the wave function of higher excited state is absolutely neglected. Thus, the subtracted constants  $\Pi_n(M_\psi)$  for these excited states might be overestimated, and as a result, the renormalized mass shifts in Ref. [6] are commonly smaller than those in our model, as one can see in the following section.

On the other hand, the wave functions of  $\psi_0$ ,  $B$  and  $C$  are needed to determine the matrix element  $\langle BC | H_{QPC} | \psi_0 \rangle$  in (15). These wave functions are usually chosen as the harmonic oscillator ones [5, 7, 19]. However, we determine them by solving the quenched mass equation Eq.(10) with Eq.(4). But for simplicity, we will neglect the corrections due to the spin-dependent potential  $V_{sd}$  to these wave function.

#### IV. NUMERICAL RESULTS AND DISCUSSION

As mentioned in Sec. I, our aim is to compare the charmonium spectra or the renormalized mass shifts

$$\Delta M_{cou} = M_{cou} - M_{que}, \quad \Delta M_{scr} = M_{scr} - M_{que}, \quad (18)$$

where the subscripts *que*, *cou*, and *scr* denote the results obtained from the quenched potential model, the coupled-channels model, and the screened potential model, respectively. The quenched mass  $M_{que}$  can be related to the bare mass  $M_0$  in the coupled-channels model by the relation:

$$M_{que} - C_{que} = M_0 - C_{cou}, \quad (19)$$

TABLE I: Charmonium spectra and mass shifts in different models in units of MeV. Here, the subscripts *que*, *cou*, and *scr* denote the results obtained from the quenched potential model, the coupled channel model, and the screened potential model, respectively. The mass shifts  $\Delta M_{cou}$  and  $\Delta M_{scr}$  are listed in the 5th and 6th columns, respectively. The results of Ref. [6] are also listed. The bare mass in the 7th column is copied from Ref. [15]. All the quantities listed here should be understood as the renormalized ones.

states	Our results					Results of Ref. [6]		
	$M_{que}$	$M_{cou}$	$M_{scr}$	$\Delta M_{cou}$	$\Delta M_{scr}$	$M'_0$	$M'_{cou}$	$\Delta M'_{cou}$
$1^1S_0$	2980	2980	2980.0	0	0	2982	2982	0
$1^3S_1$	3112	3100	3105	-12	-7	3090	3090	0
$1^1P_1$	3583	3531	3539	-52	-44	3516	3514	-2
$1^3P_0$	3476	3441	3448	-35	-28	3424	3415	-9
$1^3P_1$	3568	3520	3526	-48	-42	3505	3489	-16
$1^3P_2$	3628	3565	3577	-63	-51	3556	3550	-6
$2^1S_0$	3697	3635	3626	-62	-71	3630	3620	-10
$2^3S_1$	3754	3674	3674	-80	-80	3672	3663	-9
$1^1D_2$	3895	3818	3805	-77	-90	3799		
$1^3D_1$	3878	3794	3790	-84	-88	3785	3745	-40
$1^3D_2$	3896	3818	3805	-78	-91	3800		
$1^3D_3$	3903	3823	3812	-80	-91	3806		
$2^1P_1$	4042	3961	3909	-81	-133	3934	3929	-5
$2^3P_0$	3948	3915	3839	-33	-109	3852	3782	-70
$2^3P_1$	4030	3875	3900	-155	-130	3925	3859	-66
$2^3P_2$	4085	3966	3941	-119	-144	3972	3917	-55

where  $C_{que}$  and  $C_{cou}$  denote the renormalization constants in the quenched potential model and the coupled-channels model, respectively. Thus from Eq. (16), the mass shift  $\Delta M_{cou}$  can be given by

$$\Delta M_{cou} = -\text{Re}[\Pi(M_{cou})] - C_{que} + C_{cou}. \quad (20)$$

To improve the reliability of the calculation of the coupled-channel model, we restrict the mass region of charmonium spectrum to be below 4 GeV, in which the decays to P-wave (and higher excited)  $D$  and  $D_s$  mesons are kinematically forbidden, and only the S-wave  $D$  and  $D_s$  mesons are involved. So in the following we use the S-wave  $D_{(s)}$  mesons, of which the masses are well determined and the widths can be neglected [20], as the intermediate states only.

In the mass region below 4 GeV, the charmonium spectrum consists of the 1S, 2S, 1P, 2P and 1D levels. For convenience, we choose the renormalization condition such that the predicted  $\eta_c$  masses in the three models are fixed to be the measured value [20], i.e., 2980 MeV. Together with the inputs of the quark masses

$$m_c = 1.7 \text{ GeV}, m_q = 0.33 \text{ GeV}, m_s = 0.5 \text{ GeV}, \quad (21)$$

the renormalization condition determines the constant terms in (1):

$$C_{que} = -419 \text{ MeV}, C_{cou} = -272 \text{ MeV}, C_{scr} = -403 \text{ MeV}. \quad (22)$$

We list the numerical results of the mass spectra and the mass shifts in Tab. I. The subscripts *que*, *cou*, and *scr* denote the results obtained from the quenched potential model, the coupled channel model, and the screened

potential model, respectively. And the mass shifts have been defined in (18). In Tab. I, both  $\Delta M_{cou}$  and  $\Delta M_{scr}$  have minus sign, and on the whole, they are consistent with each other. This can also be seen from Fig. 2.

In addition, for the 1S, 2S, 1P and 1D levels, which either couple the  $D$  meson pair in P-wave or lie far away from the threshold of the  $D$  meson pair, the mass shifts  $\Delta M_{cou}$ 's are comparable to each other, which is consistent with the first Hadron Loop Theorem derived by the authors of Ref. [5] in the approximation of equal masses for charmed mesons.

However, if the  $c\bar{c}$  pair couples to  $D$  meson pair in S-wave and the mass  $M$  calculated in the coupled channel model (namely  $M_{cou}$ ) in (15) is close to the threshold  $M_B + M_C$ , the self-energy  $\Pi$ , then the mass shift  $\Delta M_{cou}$ , will strongly depend on  $M(M_{cou})$ . This is well known as the S-wave threshold effect [16], and as a result, the loop theorem [5] will be violated.

This is just the case for the 2P charmonium states, since for some of them the coupled-channel masses  $M_{cou}$  (see Tab. I) are close to the thresholds of the S-wave channels  $D\bar{D}^* + c.c.$  and  $D^*\bar{D}^{*1}$ . More in details, for the  $2^3P_0$  state ( $\chi'_{c0}$ ), the coupled-channel mass  $M_{cou}(\chi'_{c0}) = 3915$  MeV, which is fairly far from the threshold of the S-wave channels  $D\bar{D}$  and  $D^*\bar{D}^*$ . Consequently, the mass shift is as small as 33 MeV. As a second example, the coupled-

<sup>1</sup> The contributions to the mass shifts from the  $D_s^{(*)}\bar{D}_s^{(*)}$  channels are very small due to the small strange quark pair creation strength  $\gamma_s$ .

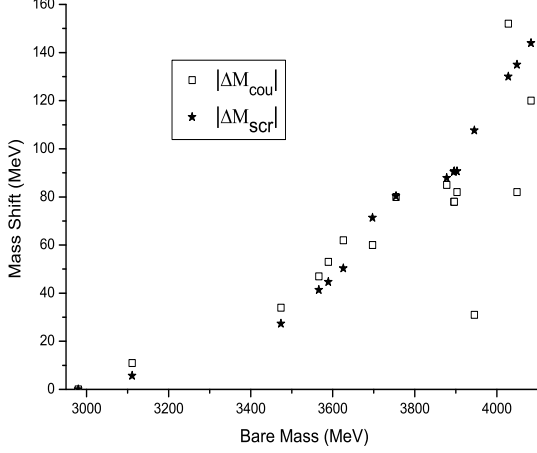


FIG. 2: Mass shifts  $\Delta M_{cou}$  and  $\Delta M_{scr}$  varying with bare mass  $M_0$ .

channel masses of the  $2^1P_1$  ( $h'_c$ ) and  $2^3P_2$  ( $\chi'_{c2}$ ) states are roughly equal. However, their mass shifts induced by the  $D^*\bar{D}^*$ , of which the threshold is closest to their coupled-channel masses, are different by a factor of 2 (see Tab. I in Ref. [5]). As a result, the mass shift of  $2^1P_1$  state is smaller than that of  $2^3P_2$  state. Finally, the coupled-channel effect of  $2^3P_1$  ( $\chi'_{c1}$ ) state should be most significant since the mass  $M_{cou}(\chi'_{c1}) = 3875$  MeV is very close to the threshold of  $D^0\bar{D}^{*0}/D^+\bar{D}^{*-} + c.c.$ . This result can also give support to the  $\chi'_{c1}$  assignment of  $X(3872)$  [21].

It needs emphasizing here that the closeness of  $M_{cou}(\chi'_{c1})$  to the threshold of  $D^0\bar{D}^{*0}$  is not very sensitive to the bare mass of  $\chi'_{c1}$ . This can be seen from Fig. 3, where the physical mass  $M_{cou}$  dependence of the unrenormalized mass shift  $-\text{Re}[\Pi(M_{cou})]$  for the  $2^3P_1$  state is shown. The relation between the unrenormalized mass shift and the renormalized one  $\Delta M_{cou}$  is given in (20). From Fig. 3 one can see the mass shift function is strongly dependent on the physical mass. As a result, the slope of the mass shift curve is very large near the threshold and "attract" the mass  $M_{cou}(\chi'_{c1})$  towards the threshold. That means, if one changes the bare mass, say, by 50 MeV, the change of the mass  $M_{cou}(\chi'_{c1})$  is only about 10-15 MeV as can be roughly found from the figure. This is just a realization of the S-wave threshold effect [16] in our coupled-channels model. More precisely, the curve in Fig. 3 shows the cusps in the neutral and charged  $D^*\bar{D}$  channels numerically (see the second paper in [16] for more discussions). Thus, the physical mass of  $\chi'_{c1}$  is quite natural to be close to the threshold of  $D^0\bar{D}^{*0}$  and thus  $\chi'_{c1}$  may be a good candidate for the  $X(3872)$  [21].

We also list the results of Ref. [6] in Tab. I for comparison. As we have mentioned, the definition of the renormalized bare mass  $M'_0$  (17) is a little different from

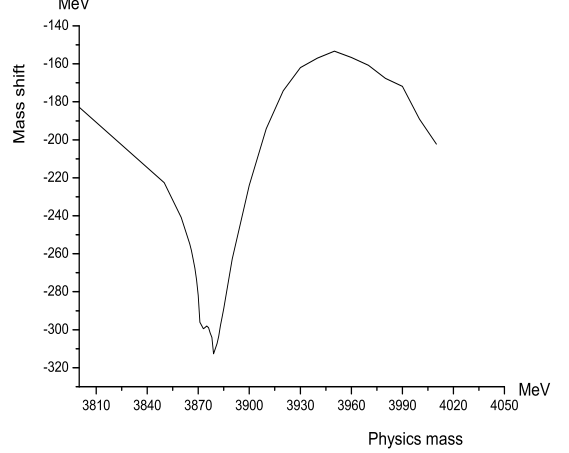


FIG. 3: The physical mass  $M_{cou}$  dependence of the unrenormalized mass shifts  $-\text{Re}[\Pi(M_{cou})]$  for the  $2^3P_1$  state.

that of  $M_0$ . Moreover, the node effect in the wave-function overlap integral for a higher excited charmonium decaying into charmed mesons is not considered in Ref. [6]. As a result, the renormalized mass shift  $\Delta M'_{cou} = \Pi(M_\psi) - \text{Re}\Pi(M)$  in [6] tends to be smaller than the one in (20) for excited states as has been analyzed in the last section. Furthermore, the authors of Ref. [6] use the available results of the quenched potential model [15], in which different parameters from ours are chosen, as their bare mass inputs (the 7th column in Tab. I). However, comparing the mass shifts in the 5th and 9th columns in Tab. I, one can find that they both have similar features as that of  $\Delta M_{scr}$ . This indicates that the screened potential in (5) depicts the main feature of the vacuum polarization effect of the dynamical quark pair creation, although it fails to describe some fine structures, such as those induced by the near S-wave threshold effects.

To compare the global features of spectra for the coupled-channel model and the screened potential model more directly, we also illustrate the c.o.g. shifts  $\Delta M^{cog}_{cou}$  and  $\Delta M^{cog}_{scr}$  in Fig. 4. Here, the c.o.g. is defined as

$$M^{cog} = \frac{M_{sig} + 3M^{cog}_{tri}}{4}, \quad (23)$$

where  $M_{sig}$  denotes the mass of the spin-singlet state, and  $M^{cog}_{tri}$  the c.o.g. of the spin-triplet states. From Fig. 4, one can see both the mass shift trajectories exhibit good behaviors, and they are roughly consistent with each other as the above analysis. However, the increase of the mass shift  $\Delta M^{cog}_{scr}$  tends to be faster than that of  $\Delta M^{cog}_{cou}$  in the higher mass region. This seems to indicate that the potential in (5) somewhat overestimates the screening effect. But it is not the whole story since the P-wave (and higher excited)  $D_{(s)}$  mesons contributions, which have been neglected, also tends to enhance

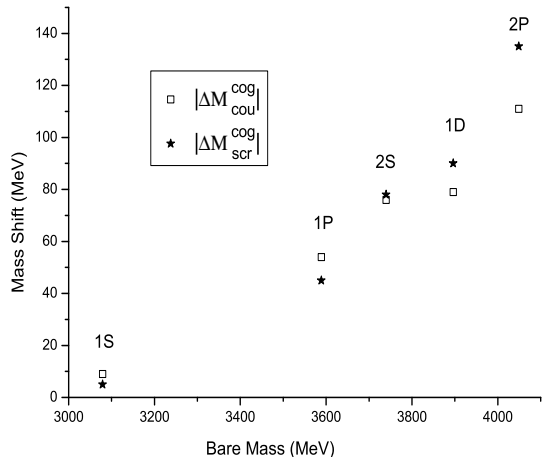


FIG. 4: The trajectories of the c.o.g. shifts  $\Delta M_{cou}^{cog}$  and  $\Delta M_{scr}^{cog}$  varying with the bare mass  $M_0$ .

the mass shift  $\Delta M_{cou}^{cog}$  in the same higher mass region.

## V. SUMMARY

We compare the charmonium spectra predicted by the coupled-channel model and the screened potential model

in the mass region below 4 GeV, in which the contributions from channels involving the P-wave (and higher excited)  $D$  and  $D_s$  mesons can be neglected. We use the same quenched limit for the two models. And for the coupled-channel model, we use the wave functions obtained by the quenched potential model in the non-relativistic limit to determine the hadronic transition matrix elements (wavefunction overlap integrals) in (15).

We find that the two models have similar global features in describing the charmonium spectrum as expected since they embody the same effect of the vacuum polarization of the dynamical quark pair creation. This agreement is encouraging for using the screened potential to further describe the mass spectrum of higher charmonium in the region above 4 GeV. Applications of both models will be helpful to clarify the nature of the newly discovered " $X, Y, Z$ " mesons [1]. In particular, we show the S-wave coupling effect on lowering the  $\chi_{c1}(2P)$  mass towards the  $D\bar{D}^*$  threshold as support to assign the  $X(3872)$  as a  $\chi_{c1}(2P)$ -dominated charmonium state.

## Acknowledgments

We thank D. Bugg for useful communications. This work was supported in part by the National Natural Science Foundation of China (No 10675003, No 10721063), and by China Postdoctoral Science Foundation (No 20080430263).

- 
- [1] S.L. Olsen, arXiv: 0801.1153 [hep-ex], to appear in Chin. Phys. C.; S. Godfrey and S.L. Olsen, Ann. Rev. Nucl. Part. Sci. **58**, 51 (2008); S.L. Zhu, arXiv:0707.2623.
  - [2] E. Eichten, K. Gottfried, T. Kinoshita, K.D. Lane and T. M. Yan, Phys. Rev. **D17**, 3090 (1978) [Erratum-ibid. **D21**, 313 (1980)]; **D21**, 203 (1980).
  - [3] K. Heikkilä, N.A. Törnqvist and S. Ono, Phys. Rev. **D29**, 110 (1984).
  - [4] A. Le Yaouanc, L. Oliver, O. Pene and J. C. Raynal, Phys. Rev. **D8**, 2223 (1973).
  - [5] T. Barnes and E.S. Swanson, Phys. Rev. **C77**, 055206 (2008).
  - [6] M.R. Pinnington and D.J. Wilson, Phys. Rev. **D76**, 077502 (2007).
  - [7] Yu. S. Kalashnikova, Phys. Rev. **D72**, 034010 (2005) [arXiv:hep-ph/0506270].
  - [8] E. Laermann, F. Langhammer, I. Schmitt and P.M. Zerwas, Phys. Lett. **B173**, 437 (1986); K.D. Born, E. Laermann, N. Pirch, T.F. Walsh and P.M. Zerwas, Phys. Rev. **D40**, 1653 (1989).
  - [9] K. T. Chao, Y. B. Ding and D. H. Qin, Commun. Theor. Phys. **18**, 321 (1992).
  - [10] Y. B. Ding, K. T. Chao and D. H. Qin, Chin. Phys. Lett. **10**, 460 (1993).
  - [11] Y. B. Ding, K. T. Chao and D. H. Qin, Phys. Rev. **D51**, 5064 (1995).
  - [12] G.S. Bali, et. al. [SESAM Collaboration], Phys. Rev. **D71**, 114513 (2005).
  - [13] A. Armoni, arXiv:0805.1339[hep-th] (to appear in Phys. Rev. D); F. Bigazzi, A.L. Cotrone, C. Núñez and A. Paredes, Phys. Rev. **D78**, 114012 (2008).
  - [14] B.Q. Li and K.T. Chao, arXiv:0903.5506.
  - [15] T. Barnes, S. Godfrey and E.S. Swanson, Phys. Rev. **D72**, 054026 (2005).
  - [16] J.L. Rosner, Phys. Rev. **D74**, 076006 (2006); D.V. Bugg, J. Phys. G **35**, 075005 (2008).
  - [17] P. Goddard, J. Goldstone, C. Rebbi and C.B. Thorn, Nucl. Phys. **B56**, 109 (1973).
  - [18] G.S. Bali, Phys. Rept. **343**, 1 (2001).
  - [19] E.S. Ackleh, T. Barnes and E.S. Swanson, Phys. Rev. **D54**, 6811 (1996).
  - [20] C.Amsler *et al.* [Particle Data Group], Phys. Lett. **B667**, 1 (2008).
  - [21] C. Meng, Y.J. Gao and K.T. Chao, arXiv: hep-ph/0506222; C. Meng and K.T. Chao, Phys. Rev. **D75**, 114002 (2007); M. Suzuki, Phys. Rev. **D72**, 114013 (2005); O. Zhang, C. Meng and H.Q. Zhang, arXiv:0901.1553.